

Article

Copolymers of 4-Trimethylsilyl Diphenyl Acetylene and 1-Trimethylsilyl-1-Propyne: Polymer Synthesis and Luminescent Property Adjustment

Tanxiao Shen ¹, Manyu Chen ¹, Haoke Zhang ^{1,2,3}, Jing Zhi Sun ^{1,2,*} and Ben Zhong Tang ^{1,4}

¹ MOE Key Laboratory of Macromolecular Synthesis and Functionalization, Department of Polymer Science and Engineering, Zhejiang University, Hangzhou 310027, China

² Centre of Healthcare Materials, Shaoxing Institute, Zhejiang University, Shaoxing 312000, China

³ Hangzhou Global Scientific and Technological Innovation Center, Zhejiang University, Hangzhou 311215, China

⁴ Shenzhen Institute of Aggregate Science and Technology, School of Science and Engineering, The Chinese University of Hong Kong, Shenzhen 518172, China

* Correspondence: sunjz@zju.edu.cn; Tel.: +86-13958091775

Abstract: Poly(4-trimethylsilyl diphenyl acetylene) (PTMSDPA) has strong fluorescence emission, but its application is limited by the effect of aggregation-caused quenching (ACQ). Copolymerization is a commonly used method to adjust the properties of polymers. Through the copolymerization of 4-trimethylsilyl diphenyl acetylene and 1-trimethylsilyl-1-propyne (TMSP), we successfully realized the conversion of PTMSDPA from ACQ to aggregation-induced emission (AIE) and aggregation-induced emission enhancement (AEE). By controlling the monomer feeding ratio and with the increase of the content of TMSDPA inserted into the copolymer, the emission peak was red-shifted, and a series of copolymers of poly(TMSDPA-*co*-TMSP) that emit blue–purple to orange–red light was obtained, and the feasibility of the application in explosive detection was verified. With picric acid (PA) as a model explosive, a super-quenching process has been observed, and the quenching constant (K_{SV}) calculated from the Stern–Volmer equation is $24,000\text{ M}^{-1}$, which means that the polymer is potentially used for explosive detection.

Keywords: copolymerization; disubstituted-acetylene; fluorescence; AIE; explosive detection



Citation: Shen, T.; Chen, M.; Zhang, H.; Sun, J.Z.; Tang, B.Z. Copolymers of 4-Trimethylsilyl Diphenyl Acetylene and 1-Trimethylsilyl-1-Propyne: Polymer Synthesis and Luminescent Property Adjustment. *Molecules* **2023**, *28*, 27. <https://doi.org/10.3390/molecules28010027>

Academic Editor: Takahiro Kusakawa

Received: 4 December 2022

Revised: 16 December 2022

Accepted: 16 December 2022

Published: 21 December 2022



Copyright: © 2022 by the authors. Licensee MDPI, Basel, Switzerland. This article is an open access article distributed under the terms and conditions of the Creative Commons Attribution (CC BY) license (<https://creativecommons.org/licenses/by/4.0/>).

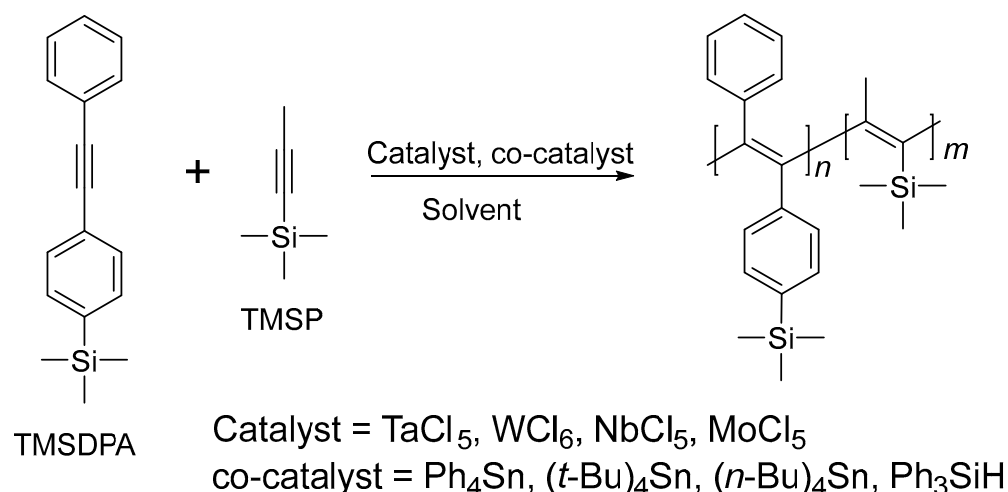
1. Introduction

Polyacetylene is a well-known conjugated polymer because of the metallic conductivity found in its highly doped films, which opened a new area of research on “synthetic metals” [1–4]. However, pristine polyacetylene is very unstable and intractable, and thereby the scope of its practical applications has been heavily limited. Replacement of the two hydrogen atoms on the acetylene monomer with appropriate substituents endows disubstituted acetylenes, and the corresponding polymers or poly(disubstituted acetylene)s (PDSAs) exhibited good stability and processability [5]. In recent years, PDSAs have shown advanced functions and promising applications in some high-tech areas, such as ultra-high gas permeability [6–8] for the transportation of small-molecule gases and solvents and luminescent elastomers for stimuli-responsive materials [9–14]. Due to the poor tolerance of polymerization catalysts to polar functional groups, however, the disubstituted acetylene monomers available for polymerization are very limited [15], which seriously restricts the related basic research and the development of new products. From the perspective of synthetic chemistry, there are mainly three ways to change the functions of polymeric materials. One is to change the polymerization reaction route so that the functional monomer can be polymerized to obtain the desired performance. However, some polymerization routes have problems to be solved, such as a long reaction time, low conversion rate and yield, etc. The second is to change the polymerization catalyst

and adjust the polymer chain structure, to obtain an improved performance. It is very difficult to develop new catalysts, and only palladium (Pd)-based catalysts [16] have been developed so far. Most PDSAs are polymerized using conventional early transition metal compounds such as WCl_6 , $MoCl_5$, $NbCl_5$, and $TaCl_5$ as catalysts. The third is to adjust the chemical composition and chain structure of the polymers by copolymerization to achieve the purpose of property modification.

Copolymerization, as one of the most commonly used modification methods, has also been reported for the preparation of PDSAs, but it is far less than that of olefin-based copolymers. The documented reports mainly focus on the two PDSAs, poly(1-trimethylsilyl-1-propyne) (PTMSP) and poly(4-trimethylsilyl diphenyl acetylene) (PTMSDPA). Since the first report of PTMSP in 1983 [17], a series of publications has appeared due to its unique structure and properties and, in particular, the extremely high gas permeability. Hamano [18] noticed that TMSP could copolymerize with other double-substituted acetylene monomers under the catalysis of $TaCl_5/Ph_3Bi$ or $NbCl_5/Ph_3Bi$, and the reaction activity sequence of monomers was obtained through the copolymerization curve: 2-octyne > TMSP > 4-octyne > 1-phenyl-1-propyne > 1-phenyl-1-hexyne. Ghisellini [19] realized the copolymerization of TMSP with 1-trimethyl-1-hexene, and the catalyst used was $TaCl_5/Ph_3Bi$. Khotimsky and colleagues [20] investigated the copolymerization of 4-methyl-2-pentyne and TMSP initiated by catalytic systems based on $NbCl_5$. PTMSDPA as a very unusual π -conjugated polymer has a polyene backbone and two side phenyl rings and is quite emissive [21] and responsive to external stimuli such as liquid solvents [22]. Kwak [23] explored PTMSDPA copolymers containing both longer and shorter alkyl side chains in the same backbone.

All the above copolymerized monomers have very similar structures, so there is great potential to regulate the property of PDSAs through copolymerization. We prepared a series of copolymers of TMSP and TMSDPA, as shown in Scheme 1. The characterization data confirmed that the resultant polymers possess the expected chemical structure, and the properties of these copolymers were investigated. We took advantage of the AIE properties of P7 to detect picric acid (PA), a model compound of nitro-aromatic explosives in aqueous media, and a high sensitivity to PA has been achieved.



Scheme 1. Synthetic route of the copolymerization of TMSP and TMSDPA.

2. Results and Discussion

2.1. Copolymerization

Copolymerization of the two monomers was conducted by using $TaCl_5-Bu_4Sn$, which was selected from seven catalysts ($TaCl_5-Bu_4Sn$, $TaCl_5-Ph_3SiH$, $NbCl_5-Ph_4Sn$, $NbCl_5-Ph_3SiH$, WCl_6-Ph_4Sn , WCl_6-Ph_3SiH , and $MoCl_5-Bu_4Sn$), because the copolymerization reaction could only proceed under this catalyst. Table 1 presents the results of the copolymerization of the monomers. The polymer yield of P1, regarded as adding a small amount

of TMSDPA to the TMSP system, was reduced to 50% of PTMSP, although the molecular weight was not significantly changed. Accordingly, it could be suggested from P4 that the reaction could not succeed once TMSP was added to TMSDPA. Further research showed that when the contents of TMSDPA reached 60% and 80%, there was no product. When TMSP reached 60% and 80%, small amounts of products could be obtained. Then, we speculated that the complex catalyst of TaCl₅-Bu₄Sn tends to polymerize TMSP.

Table 1. Copolymerization of TMSP and TMSDPA ^a.

Samples	Feed Ratio (TMSP:TMSDPA)	t (min)	Y ^b (%)	M _w ^c (×10 ⁴)	PDI ^c	Color	QY (%)
PTMSP	100:0	2	38	187.5	1.56	white	
P1	80:20	2	19	178.0	1.71	white	9.1
P2	60:40	2	13	158.6	1.93	white	10.7
P3	40:60	2	-	-	-		
P4	20:80	2	-	-	-		
PTMSDPA	0:100	2	20	233.2	1.71	yellow	25.5
P5	50:50	2	11	86.9	2.00	white	45.0
P6	50:50	4	18	111.1	1.86	white	47.1
P7	50:50	10	22	107.4	2.12	light yellow	39.1
P8	50:50	30	33	107.0	2.10	yellow	23.8
P9	50:50	50	40	146.9	2.24	yellow	9.6
P10 ^d	50:50	4	18	105.4	1.77	white	51.8
P11 ^e	50:50	4	19	106.8	1.99	white	19.8

^a Conditions: [TaCl₅] = 0.1 mmol, [Bu₄Sn] = 0.2 mmol in 6 mL toluene solution, T = 80 °C, t = time, Y = yield, PDI = poly-dispersion index, QY = quantum yield of solid. ^b The product was precipitated from methanol/acetone (v/v, 5/1). ^c Estimated by GPC of the THF-soluble part against polystyrene calibration. ^d TMSP is added first, and TMSDPA is added after 2 min. ^e TMSDPA is added first, and TMSP is added after 2 min.

We also examined the time effect of the polymerization reaction. The molecular weight reached 10⁶ even though the reaction time was only 2 min for the homo-polymerization of TMSP and TMSDPA. Gel was produced when the reaction time was extended to 10 min. The results indicate that the catalyst has very high activity in the homo-polymerization of TMSP and TMSDPA. The product yield improved with the increase of the reaction time, but the molecular weight was almost unchanged, as suggested by the comparison between P5 and P9. These results indicate that the initiation of the active center is the rate-determining step in polymerization, and the chain growth rate is extremely high. The results of P10 and P11 show that the yield and molecular weight of the polymer were not significantly affected by changing monomer sequences.

2.2. Structural Characterization

FTIR and ¹H NMR spectroscopic techniques were employed to confirm the chemical structure of the polymers. We used the characterization data of P7 as representative of the copolymer to compare with the homopolymer. Other copolymers have similar data (Supplementary Materials: Figures S1–S3). As clearly shown in the FTIR spectra (Figure 1), the absorption band around 2200 cm⁻¹ that could be attributed to the tensile vibration of the C≡C bond was absent. At the same time, a new asymmetric absorption band near 1600 cm⁻¹ appeared, which can be assigned to the asymmetric stretching vibration peak of the C=C bond. The changes of these two characteristic bands indicate the complete consumption of the triple bond and transformation into the double bond after the polymerization reaction. Infrared absorption spectra were used to further characterize the influence of the reaction time on the polymer composition (Figure S3). The overall infrared spectrum changes showed a trend of superposition of PTMSP and PTMSDPA spectra with the reaction time. The absorption band of 1120 cm⁻¹ assigned as the respiratory vibration of the benzene ring appeared in the infrared spectrum since P8, indicating that the TMSDPA component in the copolymer increased with the increase of time.

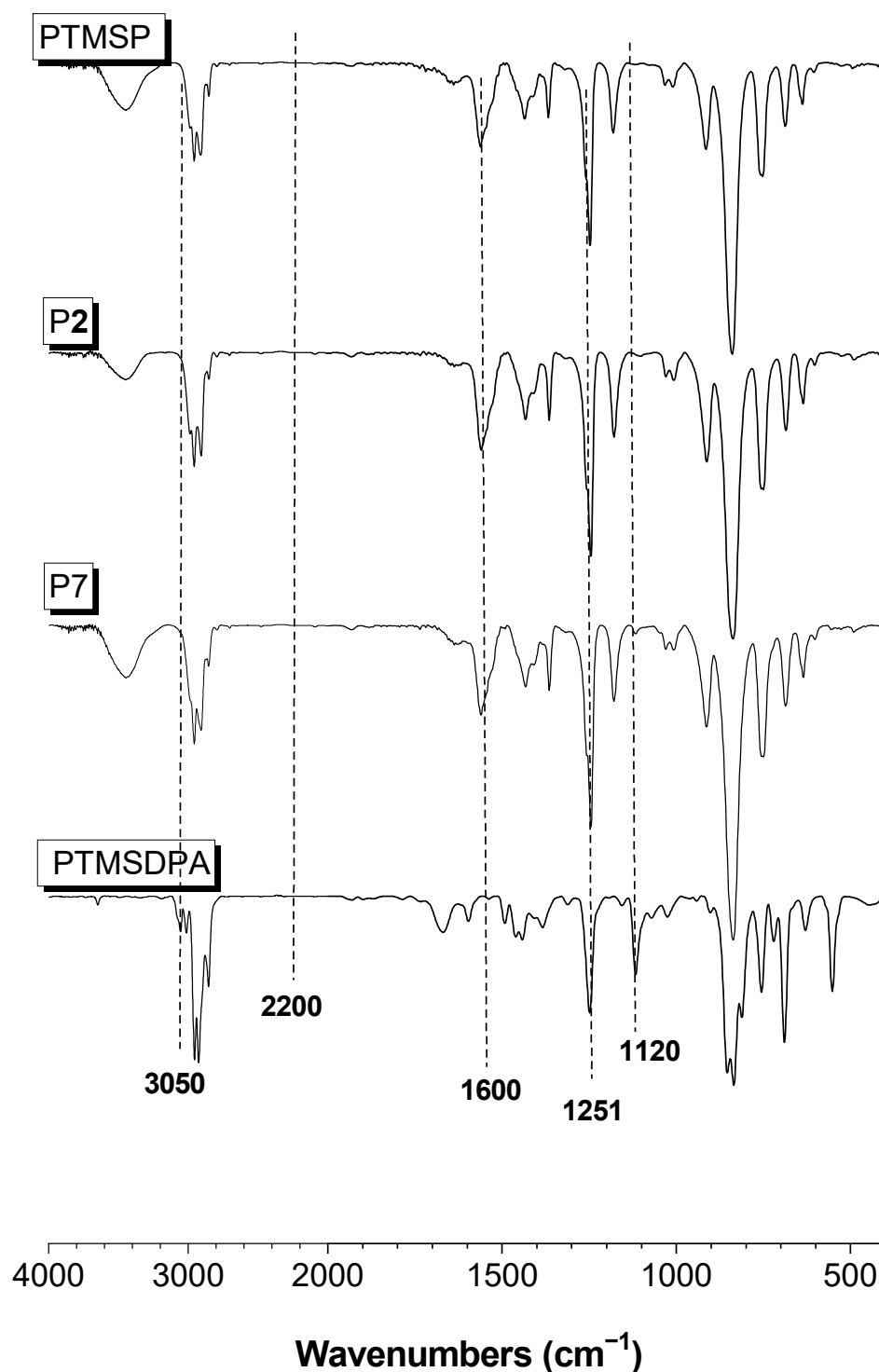


Figure 1. FTIR spectra of PTMSP, P2, P7, and PTMSDPA in KBr pellets.

Further evidence comes from the ¹H NMR spectra (Figure 2) of PTMSP, P7, and PTMSDPA. The signal in the low-field part of the spectrum was amplified for analysis. The resonant peak around 7.5 ppm, which was assigned to the protons of the benzene ring, existed in P7. The monomer showed a sharp resonance signal around 0.1 ppm, which was assigned to the protons of methyl and transformed into a dull band. The above results suggest that copolymerization of phenyl disubstituted acetylene and alkyl-silyl disubstituted acetylene has been successfully achieved.

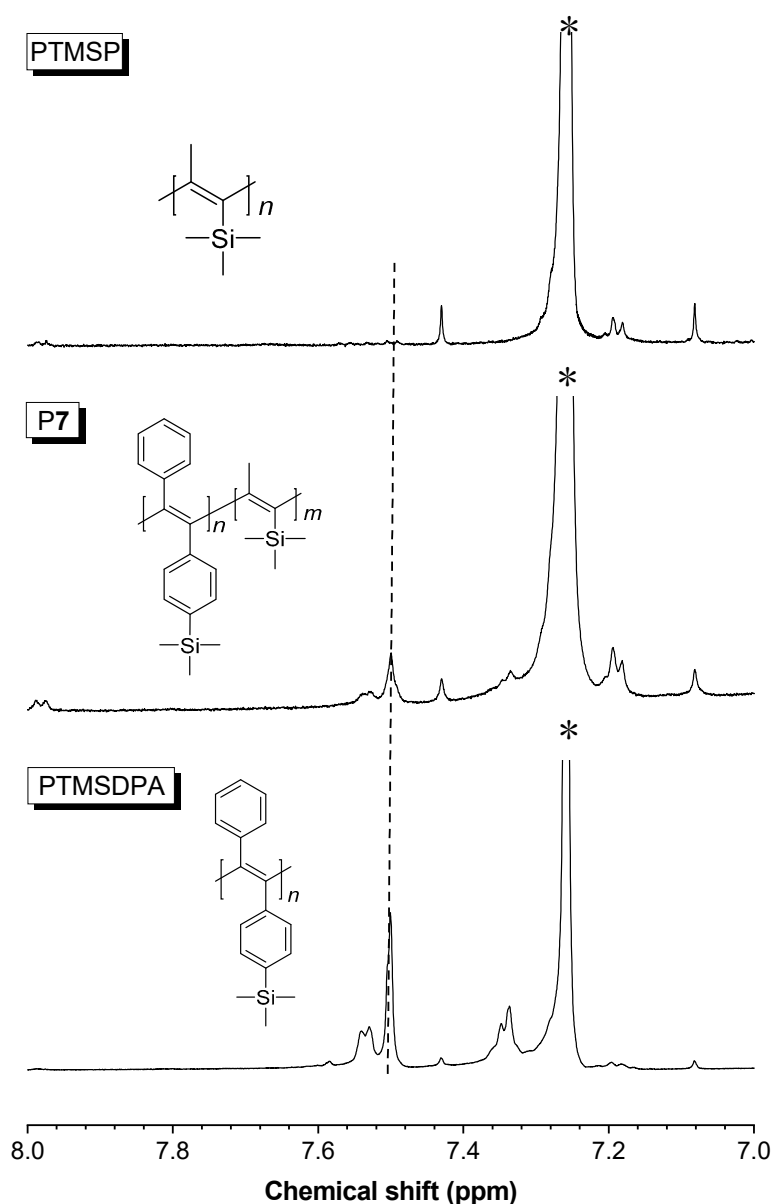


Figure 2. ^1H NMR spectra of PTMSP, P7, and PTMSDPA (CDCl_3). The asterisks represent solvent peaks.

2.3. Photophysical Property

Poly-diphenyl acetylenes are highly emissive even in a solid state since the introduction of the benzene ring changes the electronic structure of the backbone, and the fluorescence property of PTMSDPA has been widely reported [24–28]. Since no one has tried to synthesize copolymers containing PTMSDPA chain segments, the absorption and emission properties of these copolymers have never been reported anywhere. Figure 3a shows the UV-visible absorption spectra of copolymers.

A straight line in the range from 370 to 620 nm of PTMSP was recorded, and this observation is consistent with the appearance of the white powder. This means that the polymer does not have the extended electronic structure of general polyacetylenes, because the large substituents distort the conjugation of the polyene backbone. PTMSDPA has two obvious absorption peaks at 430 and 375 nm, respectively. The absorption band of 430 nm can be assigned to the $\pi\text{-}\pi^*$ transition of the conjugated backbone of the polymer, and the absorption band of 375 nm can be assigned to the $\pi\text{-}\pi^*$ transition of the diphenylethylene conjugated unit. There are no characteristic absorption peaks of 375 nm

and 430 nm assigned to PTMSDPA in P1 and P2, indicating that P1 and P2 contain few or no diphenylethylene conjugate units, and this is consistent with the results of structural characterization. P5 and P6 still do not show the characteristic absorption band at 430 nm, suggesting that it is difficult to link the TMSDPA monomer to the PTMSP chain end when the reaction time is short. P7 shows the character of PTMSDPA's UV absorption peak. This indicates that when the reaction time is prolonged to a sufficient degree, the TMSP monomer is consumed and the active center begins to accept the introduction of TMSDPA, resulting in the occurrence of PTMSDPA fragments in the polymer chain. As a result, the UV-visible absorption spectrum of the polymer shows the characteristic absorption band of its homopolymer. The UV-visible absorption spectra of the polymer P8 and P9 were more obvious by prolonging the polymerization time to 30 and 50 min, which indicates that there are already enough PTMSDPA segments in the polymers. Compared with P10, the stronger UV absorption peak of P11 (Figure S5) at 415 nm indicates that there are more TMSDPA fragments in the main chain, which further indicates that it is difficult for TMSDPA to insert into the PTMSP chain.

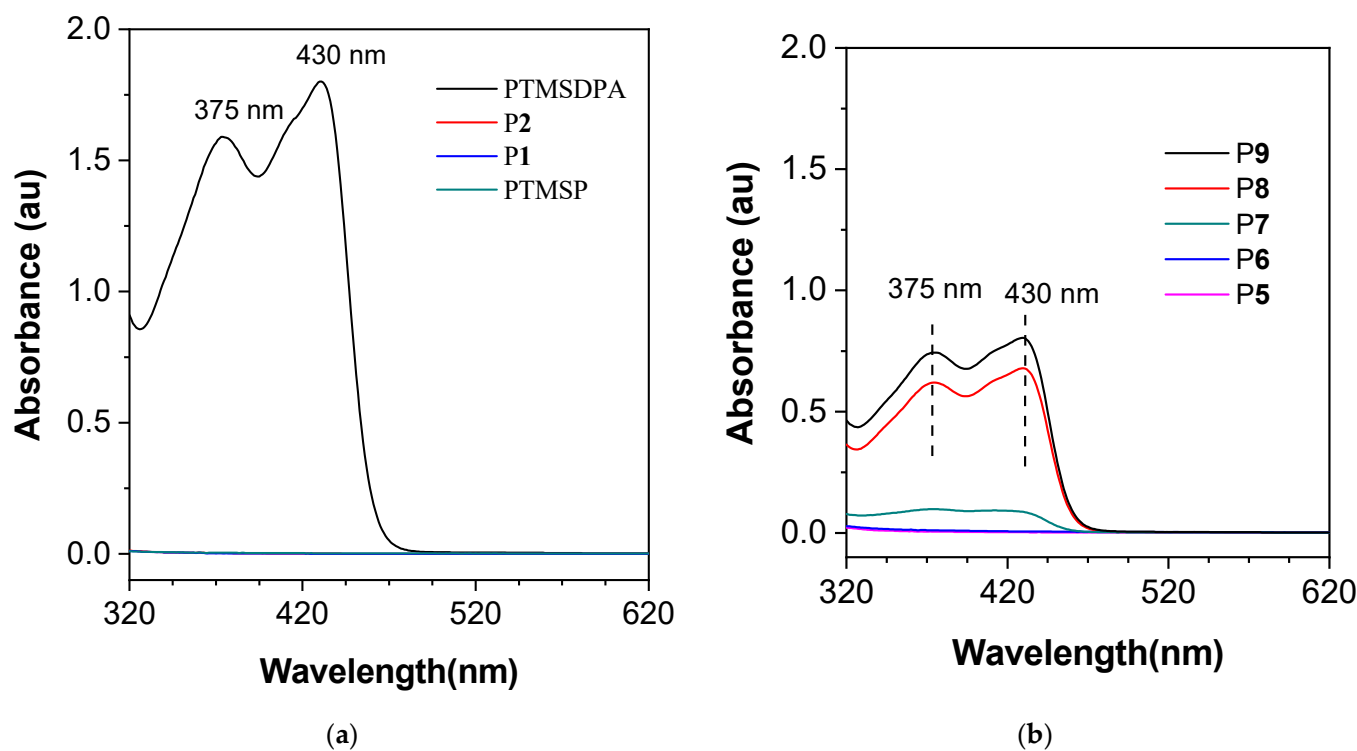


Figure 3. (a) UV-vis spectra of PTMSP, P1, P2, and PTMSDPA. (b) UV-vis spectra of P5, P6, P7, P8, and P9.

The above deduction was supported by the experimental data shown in Figure 4. The PTMSP was non-emissive in THF solution, and a strong luminescence peak of 498 nm appeared in the photoluminescence (PL) spectrum of PTMSDPA. The PL spectrum of P1 almost overlaps with PTMSP. However, P2 shows a weak luminescence peak at around 490 nm, indicating that the copolymerization was successful. This is inconsistent with the previous results because fluorescence spectra are more sensitive than FTIR, ^1H NMR, and UV-visible absorption spectra. P7–P9 solutions showed gradually enhanced fluorescence emission. The red-shift fluorescence emission peak of P11 (Figure S6) compared with P10 confirmed our previous results. The luminescent performance of P5 and P6 looks abnormal: their dilute solutions have not shown absorption and emission bands, which implies that there are no TMSDPA segments in polymers. However, their powders emit fluorescence under UV light (Figure S7). This phenomenon can be associated with the aggregation-induced emission (AIE) effect. For a typical AIE molecule or macromolecule, there is no or

very weak luminescent emission observed for the dilute solution of a good solvent, however significantly enhanced luminescent emission can be recorded when the molecules form aggregates or are trapped in a certain cramped environment [29–32]. Tetraphenylethylene (TPE) is a representative AIE-active luminogen (AIEgen), and the structure for the main chain of poly(TMSP-co-TMSDPA) containing two adjacently inserted TMSDPA units is similar to that of TPE. The absence of fluorescence emission of P6 in the solution state does not mean the absence of TMSDPA units in the polymer chain but it indicates that there are very short segments of TMSDPA in the polymer chain, serving as the source of the AIE property.

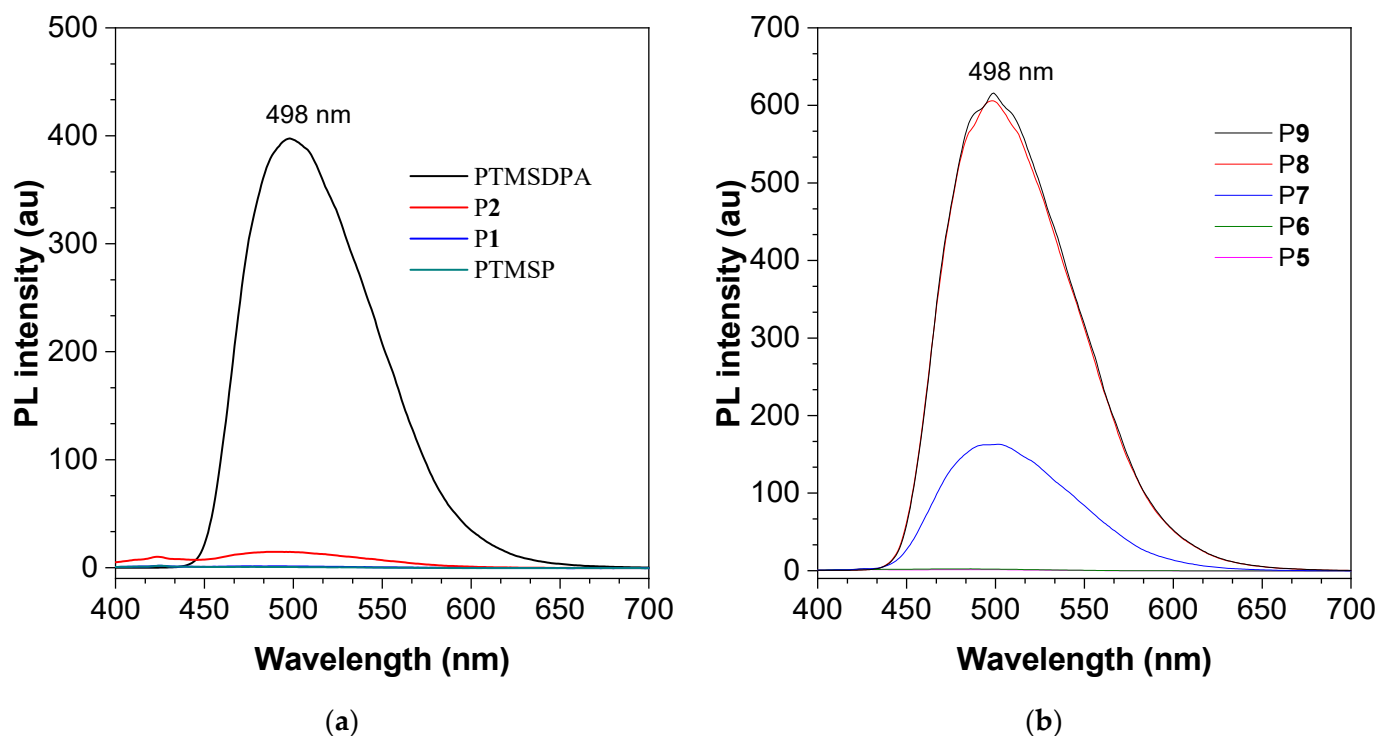


Figure 4. (a) PL spectra of PTMSP, P1, P2, and PTMSDPA. (b) PL spectra of P5, P6, P7, P8, and P9.

The fluorescence spectra (Figure 5) of solid powders of polymers P5–P9 were measured to verify the above deduction. The solid powders of P5 and P6 both emitted blue fluorescence with a peak at around 470 nm when a larger ratio of TMSDPA monomer was introduced into the polymer chain with the extension of the polymerization time, and the PTMSDPA segments were lengthened. Consequently, the emission spectrum was red-shifted. The emission peaks of P7–P9 solids appeared at 545, 555, and 558 nm, respectively. According to the classical method to verify the AIE properties of molecules, the PL behavior of the polymers in the mixed solvent system of THF/H₂O with different water contents was analyzed by using THF as a good solvent and water as a bad solvent (Figures 6, S8 and S9). The excitation wavelength of 375 nm was chosen to avoid the effect of Raman scattering by water. Figure 6 shows that with the increase of the water fraction in the mixed solvent, the system changed from non-luminescent to luminous, and the fluorescence intensity increased with the increase of the water content, which fully confirms that P6 is an AIE-type polymer. There was weak fluorescence in the P7 solution. The fluorescence was gradually enhanced when water, the poor solvent of P7, was added to the solution, and the solution reached the highest fluorescence intensity when the water fraction reached 90%. The polymer exhibits typical AEE behavior.

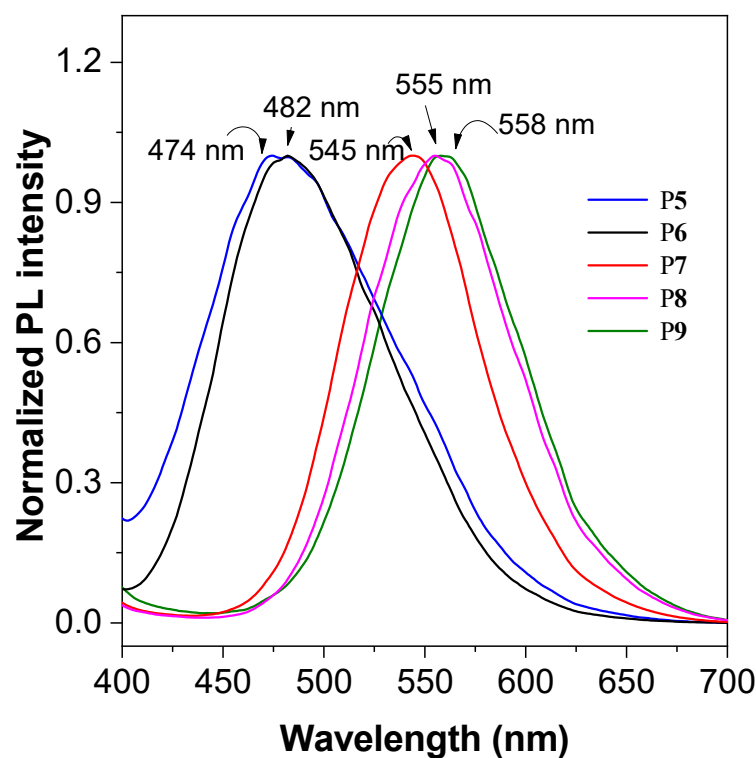


Figure 5. PL spectra of P7, P8, P9, P10, and P11 powders. $\lambda_{\text{ex}} = 375 \text{ nm}$.

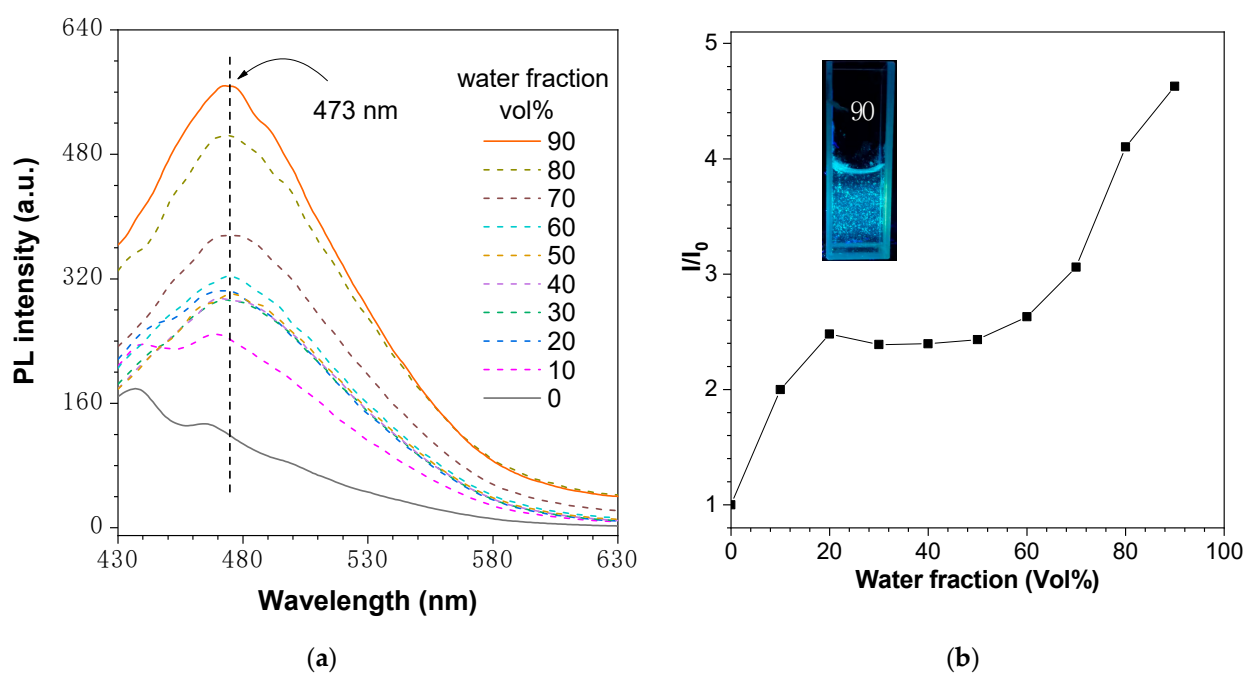


Figure 6. (a) PL behavior of P6 in THF/water mixtures with different water fractions (f_w). (b) Plot of peak intensity of P6 in THF/water mixtures with different water fractions. I_0 = Peak intensity of P6 when $f_w = 0$. I = Peak intensity of P6 when $f_w = 0$. $\lambda_{\text{ex}} = 375 \text{ nm}$, Concentration = $100 \mu\text{M}$. Inset: Photographs of the fluorescence of P6 in THF/water mixtures with a 90% water fraction.

On the other hand, PTMSDPA shows a typical ACQ behavior (Figure S9). The fluorescence intensity decreased with the increase of water fraction, which is similar to the luminescence behavior of most diphenyl acetylene derivatives [21–25]. According to the above results, a series of copolymers containing different lengths of PTMSDPA can be

obtained by controlling the proportion of the two monomers and the reaction time. We can not only regulate the luminescence color from blue–purple to orange–red, but we can also adjust the luminescent behavior from ACQ of the homopolymer PTMSDPA to AIE of the copolymer.

2.4. Explosive Detection

Detection of explosives has drawn much attention because of its application in global safety and anti-terrorism activities. In this area, fluorescence spectroscopy has been widely used due to its high sensitivity, good selectivity, low cost, and easy operation. The suspension formed by P7 in the mixed solvent shows high stability compared with the suspension formed by small molecules and can be placed for several months without precipitation, which makes the system more suitable for working as a detection medium. Then, P7 in the THF/water mixture with a 90% water fraction was used as the fluorescent detection medium, and picric acid (PA, 2,4,6-trinitrophenol) was chosen as a model of explosive to simulate practical detection. As shown in Figure 7a, the intensity of the fluorescence began to decrease with the addition of more and more PA into the suspension, but the maximum emission wavelength did not change. In the PA concentration range of 0–100 μM , an exponential growth (I_0/I vs. PA concentration) can be derived (Figure 7b), which implies that the detection system has a super-amplification effect, as observed in other AIE-active polymer systems [33–41]. Based on the experimental data, the quenching constant (K_{SV}) of PA to P7 was calculated from the Stern–Volmer plot, which is as high as $24,000 \text{ M}^{-1}$. This attempt suggests that P7 is potentially used as an effective fluorescent probe in the fabrication of test plates and/or portable sensors for explosive detection.

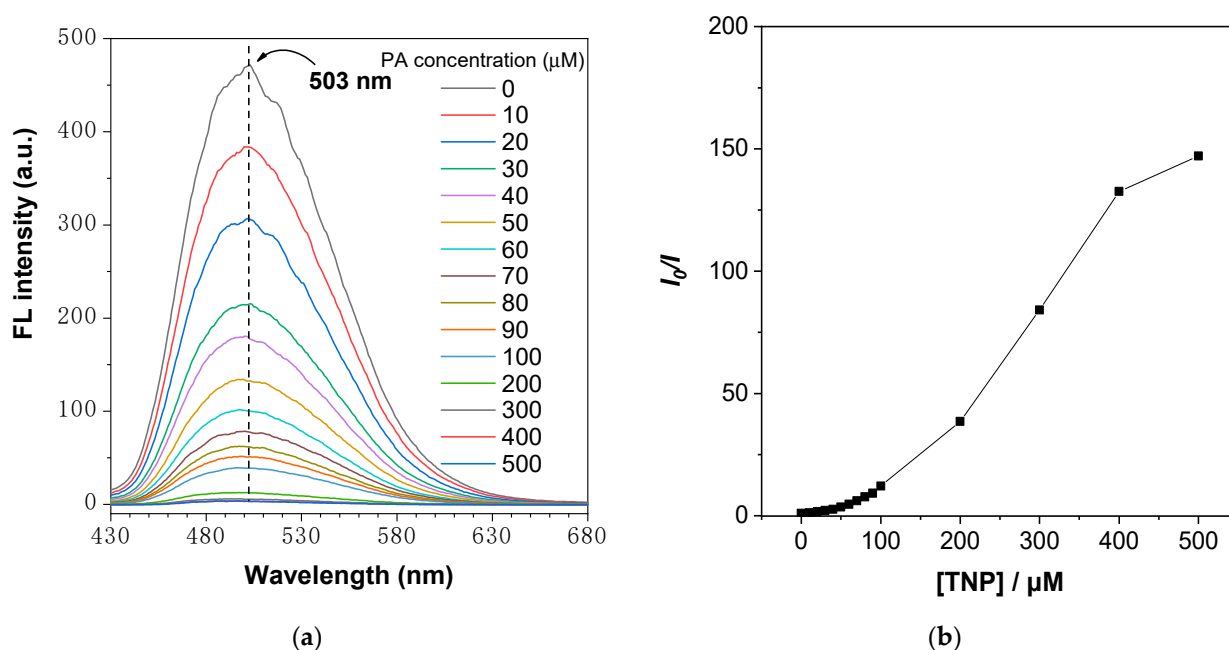


Figure 7. (a) PL spectra of P7 in THF/H₂O (90%) solution with different amounts of PA. (b) Stern–Volmer plot of I_0/I vs. PA concentration in THF/H₂O (90%) solution. I_0 and I are the peak PL intensity at $[\text{TNP}] = 0 \text{ mM}$ and a non-zero concentration. $[\text{M}]$: 10 μM , $\lambda_{\text{ex}} = 387 \text{ nm}$.

3. Materials and Methods

3.1. Materials

The 1-Trimethylsilyl-1-propyne (TMSP) and TaCl₅ were purchased from J&K Scientific (Beijing, China). Bu₄Sn, Ph₄Sn, Ph₃SiH, and Et₃SiH were purchased from Energy Chemical (Shanghai, China). WCl₆, MoCl₅, and NbCl₅ were purchased from Sigma-Aldrich Corporation (Shanghai, China). The 4-Trimethylsilyl diphenyl acetylene (TMSDPA) was purchased from Tokyo Chemical Industry (Shanghai, China). All the chemicals were used directly

without further purification. Tetrahydrofuran (THF) and toluene were freshly distilled from sodium and benzophenone ketyl under nitrogen and normal pressure.

3.2. Instruments

The molecular weight (M_w and M_n) and polydispersity (M_w/M_n) of the polymers were estimated in THF using a gel permeation chromatography (GPC, PL-GPC-50, Waters Corporation, Milford, CT, USA) system with a set of monodisperse polystyrene standards covering the molecular weight varying from 10^3 to 10^7 as calibration. FTIR spectra were recorded on a VECTOR 22 (Bruker Corporation, Billerica, MA, USA) spectrometer. ^1H NMR spectra were recorded on AVANCE III 400 (Bruker Corporation, Billerica, MA, USA) spectrometers, and tetramethylsilane (TMS) was used as an internal standard. UV-vis absorption spectra were recorded on a Varian CARY 100 Bio UV-vis (Agilent Technologies Inc, Santa Clara, CA, USA) spectrophotometer. Fluorescence spectra were recorded on a RF-5301PC (Shimadzu, Kyoto, Japan) spectrofluorophotometer. Quantum yield was recorded on the Spectrofluorometer FS5 (Edinburgh Instruments, Livingston, Scotland, UK) spectrofluorophotometer.

3.3. Polymer Synthesis

The polymerizations were carried out under the protection of dry nitrogen using the standard glovebox or Schlenk technique, except for polymer purification. The catalyst (1 eq., 1.0 mmol) and co-catalysts (2 eq., 2.0 mmol) were stirred with 400 rpm in a desired solution (3 mL) at $80\text{ }^\circ\text{C}$ for 20 min, and then 3 mL of toluene solution of the monomers (10 eq., 10 mmol) was added. The mixture was stirred at $80\text{ }^\circ\text{C}$ for the desired period of time and the reaction was quenched with nearly 8–10 mL of methanol and washed with 120 mL of methanol and acetone three times to precipitate a solid polymer. Then, the solid sample was filtered by a filter funnel with a fritted disc and dried under a vacuum for 24 h.

4. Conclusions

In this article, copolymers of disubstituted acetylenes containing both phenyl and alkylsilyl in the same backbone were synthesized and the chemical structures of the resultant polymers were characterized with FTIR and NMR spectroscopy techniques. Their emission properties varied according to the proportion of the two monomers. A higher content of TMSDPA units in the copolymers led to significantly enhanced, red-shifted emission in the solid and solution, and polymers were adjusted from ACQ to AIE copolymers. Consequently, it was possible to finely tune the emission properties of the polymers simply via the copolymerization of monomers. Moreover, using the P7 suspension and PA as the detection medium and model explosive, a super-quenching process has been observed and a good linear relationship between $\ln(I_0/I)$ vs. PA has been established. The quenching constant (K_{SV}) calculated using the Stern–Volmer equation was $24,000\text{ M}^{-1}$. This result is expected to be quite helpful in the molecular design of light-emitting materials with finely tuned fluorescence emission and in the further research of poly(disubstituted acetylene) derivatives.

Supplementary Materials: The following supporting information can be downloaded at: <https://www.mdpi.com/article/10.3390/molecules28010027/s1>. Figure S1: FTIR spectra of TMS, PTMS, TMSDPA, and PTMSDPA in KBr pellets. Figure S2: FTIR spectra of PTMS, P1, P2, and PTMSDPA in KBr pellets. Figure S3: FTIR spectra of P5, P6, P7, P8, and P9 in KBr pellets. Figure S4: ^1H NMR spectra of PTMS, P7, and PTMSDPA (CDCl_3). Figure S5: UV-vis spectra of P10 and P11 in THF solution. Figure S6: PL spectra of P10 and P11 powders. Figure S7: Fluorescence photos of P6 in THF solution and powder under 365 nm light. Figure S8: PL behavior of P7 in THF/water mixtures. Figure S9: PL behavior of PTMSDPA in THF/water mixtures. Table S1: The quantum yield for the suspensions of PTMSDPA, P6 and P7.

Author Contributions: Investigation, methodology, data curation, and writing—original draft preparation, T.S. and M.C.; software and figure improvement H.Z.; conceptualization, methodology, supervision, project administration, and funding acquisition, J.Z.S.; supervision and funding acquisition, B.Z.T. All authors have read and agreed to the published version of the manuscript.

Funding: This research was funded by the National Natural Science Foundation of China (22021715 and 21490571).

Institutional Review Board Statement: Not applicable.

Informed Consent Statement: Not applicable.

Data Availability Statement: Not applicable.

Acknowledgments: This work was partially supported by the Youth Talent Excellence Program of ZJU-Hangzhou Global Scientific and Technological Innovation Center.

Conflicts of Interest: The authors declare no conflict of interest.

References

1. Shirakawa, H.; Louis, E.J.; MacDiarmid, A.G.; Chiang, C.K.; Heeger, A.J. Synthesis of electrically conducting organic polymers: Halogen derivatives of polyacetylene, $(\text{CH})_x$. *J. Chem. Soc. Chem. Commun.* **1977**, *16*, 578–580. [[CrossRef](#)]
2. Shirakawa, H. The discovery of polyacetylene film: The dawning of an era of conducting polymers (nobel lecture). *Angew. Chem. Int. Ed.* **2001**, *40*, 2575–2580. [[CrossRef](#)]
3. MacDiarmid, A.G. “Synthetic metals”: A novel role for organic polymers (nobel lecture). *Angew. Chem. Int. Ed.* **2001**, *40*, 2581–2590. [[CrossRef](#)]
4. Heeger, A.J. Semiconducting and metallic polymers: The fourth generation of polymeric materials (nobel lecture). *Angew. Chem. Int. Ed.* **2001**, *40*, 2591–2611. [[CrossRef](#)]
5. Lam, J.W.Y.; Tang, B.Z. Functional polyacetylenes. *Acc. Chem. Res.* **2005**, *38*, 745–754. [[CrossRef](#)] [[PubMed](#)]
6. Hu, Y.; Shiotsuki, M.; Sanda, F.; Freeman, B.D.; Masuda, T. Synthesis and properties of indan-based polyacetylenes that feature the highest gas permeability among all the existing polymers. *Macromolecules* **2008**, *41*, 8525–8532. [[CrossRef](#)]
7. Nagai, K.; Masuda, T.; Nakagawa, T.; Freeman, B.D.; Pinnau, I. Poly 1-(trimethylsilyl)-1-propyne and related polymers: Synthesis, properties and functions. *Prog. Polym. Sci.* **2001**, *26*, 721–798. [[CrossRef](#)]
8. Tsuchihara, K.; Masuda, T.; Higashimura, T. Tractable silicon-containing poly(diphenylacetylenes)—Their synthesis and high gas-permeability. *J. Am. Chem. Soc.* **1991**, *113*, 8548–8549. [[CrossRef](#)]
9. Han, D.C.; Jin, Y.J.; Lee, J.H.; Kim, S.I.; Kim, H.J.; Song, K.H.; Kwak, G. Environment-specific fluorescence response of microporous, conformation-variable conjugated polymer film to water in organic solvents: On-line real-time monitoring in fluidic channels. *Macromol. Chem. Phys.* **2014**, *215*, 1068–1076. [[CrossRef](#)]
10. Jin, Y.J.; Bae, J.E.; Cho, K.S.; Lee, W.E.; Hwang, D.Y.; Kwak, G. Room temperature fluorescent conjugated polymer gums. *Adv. Funct. Mater.* **2014**, *24*, 1928–1937. [[CrossRef](#)]
11. Lee, W.E.; Jin, Y.J.; Kim, S.I.; Kwak, G.; Kim, J.H.; Sakaguchi, T.; Lee, C.L. Fluorescence turn-on response of a conjugated polyelectrolyte with intramolecular stack structure to biomacromolecules. *Chem. Commun.* **2013**, *49*, 9857–9859. [[CrossRef](#)] [[PubMed](#)]
12. Jin, Y.J.; Kwak, G. Unusual, highly efficient fluorescence emission enhancement of conjugated polymers with an intramolecular stack structure through thermal annealing at high temperature. *Macromolecules* **2017**, *50*, 9846–9851. [[CrossRef](#)]
13. Kwak, G.; Fukao, S.; Fujiki, M.; Sakaguchi, T.; Masuda, T. Temperature-dependent, static, and dynamic fluorescence properties of disubstituted acetylene polymer films. *Chem. Mater.* **2006**, *18*, 2081–2085. [[CrossRef](#)]
14. Lee, W.E.; Lee, C.L.; Sakaguchi, T.; Fujiki, M.; Kwak, G. Piezochromic fluorescence in liquid crystalline conjugated polymers. *Chem. Commun.* **2011**, *47*, 3526–3528. [[CrossRef](#)] [[PubMed](#)]
15. Liu, J.Z.; Lam, J.W.Y.; Tang, B.Z. Acetylenic polymers: Syntheses, structures, and functions. *Chem. Rev.* **2009**, *109*, 5799–5867. [[CrossRef](#)]
16. Yang, F.L.; Zhang, S.J.; Shen, T.X.; Ni, J.C.; Zhang, J.; Cheng, X.; Sun, J.Z.; Fu, Z.S.; Tang, B.Z. Polymerization of 1-chloro-2-phenylacetylene derivatives by using a brookhart-type catalyst. *Polym. Chem.* **2019**, *10*, 4801–4809. [[CrossRef](#)]
17. Masuda, T.; Isobe, E.; Higashimura, T.; Takada, K. Poly[1-(trimethylsilyl)-1-propyne]- a new high polymer synthesized with transition-metal catalysts and characterized by extremely high gas-permeability. *J. Am. Chem. Soc.* **1983**, *105*, 7473–7474. [[CrossRef](#)]
18. Hamano, T.; Masuda, T.; Higashimura, T. Polymerization of silicon-containing acetylenes. 8. Copolymerization of 1-(trimethylsilyl)-1-propyne with disubstituted hydrocarbon acetylenes. *J. Polym. Sci. Part A Polym. Chem.* **1988**, *26*, 2603–2612. [[CrossRef](#)]
19. Ghisellini, M.; Quinzi, M.; Baschetti, M.G.; Doghieri, F.; Costa, G.; Sarti, G.C. Sorption and diffusion of vapors in ptmsp and ptmsp/ptmse copolymers. *Desalination* **2002**, *149*, 441–445. [[CrossRef](#)]

20. Sultanov, E.Y.; Ezhov, A.A.; Shishatskiy, S.M.; Buhr, K.; Khotimskiy, V.S. Synthesis, characterization, and properties of poly(1-trimethylsilyl-1-propyne)-block-poly(4-methyl-2-pentyne) block copolymers. *Macromolecules* **2012**, *45*, 1222–1229. [[CrossRef](#)]
21. Jin, Y.J.; Kwak, G. Properties, functions, chemical transformation, nano-, and hybrid materials of poly(diphenylacetylene)s toward sensor and actuator applications. *Polym. Rev.* **2016**, *57*, 175–199. [[CrossRef](#)]
22. Kwak, G.; Lee, W.E.; Jeong, H.; Sakaguchi, T.; Fujiki, M. Swelling-induced emission enhancement in substituted acetylene polymer film with large fractional free volume: Fluorescence response to organic solvent stimuli. *Macromolecules* **2009**, *42*, 20–24. [[CrossRef](#)]
23. Lee, W.E.; Han, D.C.; Sakaguchi, T.; Kim, Y.B.; Lee, C.L.; Kwak, G. Finely tuned fluorescence emission of polydiphenylacetylene films obtained by copolymerization. *Macromol. Chem. Phys.* **2012**, *213*, 2293–2298. [[CrossRef](#)]
24. Kwak, G.; Minakuchi, M.; Sakaguchi, T.; Masuda, T.; Fujiki, M. Alkyl side-chain length effects on fluorescence dynamics, lamellar layer structures, and optical anisotropy of poly(diphenylacetylene) derivatives. *Macromolecules* **2008**, *41*, 2743–2746. [[CrossRef](#)]
25. Lee, W.E.; Lee, C.L.; Sakaguchi, T.; Fujiki, M.; Kwak, G. Fluorescent viscosity sensor film of molecular-scale porous polymer with intramolecular pi-stack structure. *Macromolecules* **2011**, *44*, 432–436. [[CrossRef](#)]
26. Lee, W.E.; Oh, C.J.; Kang, I.K.; Kwak, G. Diphenylacetylene polymer nanofiber mats fabricated by freeze drying: Preparation and application for explosive sensors. *Macromol. Chem. Phys.* **2010**, *211*, 1900–1908. [[CrossRef](#)]
27. Lee, W.E.; Oh, C.J.; Park, G.T.; Kim, J.W.; Choi, H.J.; Sakaguchi, T.; Fujiki, M.; Nakao, A.; Shinohara, K.-I.; Kwak, G. Substitution position effect on photoluminescence emission and chain conformation of poly(diphenylacetylene) derivatives. *Chem. Commun.* **2010**, *46*, 6491. [[CrossRef](#)]
28. Kim, S.I.; Jin, Y.J.; Lee, W.E.; Yu, R.; Park, S.J.; Kim, H.J.; Song, K.H.; Kwak, G. Microporous conjugated polymers with enhanced emission in immiscible two-phase system in response to surfactants. *Adv. Mater. Interfaces* **2014**, *1*, 7. [[CrossRef](#)]
29. Shen, X.Y.; Wang, Y.J.; Zhao, E.G.; Yuan, W.Z.; Liu, Y.; Lu, P.; Qin, A.J.; Ma, Y.G.; Sun, J.Z.; Tang, B.Z. Effects of substitution with donor-acceptor groups on the properties of tetraphenylethene trimer: Aggregation-induced emission, solvatochromism, and mechanochromism. *J. Phys. Chem. C* **2013**, *117*, 7334–7347. [[CrossRef](#)]
30. Wang, Y.J.; Li, Z.Y.; Tong, J.Q.; Shen, X.Y.; Qin, A.J.; Sun, J.Z.; Tang, B.Z. The fluorescence properties and aggregation behavior of tetraphenylethene-perylenebisimide dyads. *J. Mater. Chem. C* **2015**, *3*, 3559–3568. [[CrossRef](#)]
31. Wang, X.; Wang, W.J.; Wang, Y.M.; Sun, J.Z.; Tang, B.Z. Poly(phenylene-ethynylene-alt-tetraphenylethene) copolymers: Aggregation enhanced emission, induced circular dichroism, tunable surface wettability and sensitive explosive detection. *Polym. Chem.* **2017**, *8*, 2353–2362. [[CrossRef](#)]
32. Xue, J.Q.; Bai, W.; Duan, H.Y.; Nie, J.J.; Du, B.Y.; Sun, J.Z.; Tang, B.Z. Tetraphenylethene cross-linked thermosensitive microgels via acylhydrazone bonds: Aggregation-induced emission in nanoconfined environments and the cononsolvency effect. *Macromolecules* **2018**, *51*, 5762–5772. [[CrossRef](#)]
33. Dong, W.Y.; Fei, T.; Palma, A.; Scherf, U. Aggregation induced emission and amplified explosive detection of tetraphenylethylene-substituted polycarbazoles. *Polym. Chem.* **2014**, *5*, 4048–4053. [[CrossRef](#)]
34. Li, D.D.; Zhang, Y.P.; Fan, Z.Y.; Yu, J.H. Aie luminogen-functionalised mesoporous nanomaterials for efficient detection of volatile gases. *Chem. Commun.* **2015**, *51*, 13830–13833. [[CrossRef](#)] [[PubMed](#)]
35. Li, Q.Y.; Ma, Z.; Zhang, W.Q.; Xu, J.L.; Wei, W.; Lu, H.; Zhao, X.S.; Wang, X.J. Aie-active tetraphenylethene functionalized metal-organic framework for selective detection of nitroaromatic explosives and organic photocatalysis. *Chem. Commun.* **2016**, *52*, 11284–11287. [[CrossRef](#)]
36. Shyamal, M.; Maity, S.; Mazumdar, P.; Sahoo, G.P.; Maity, R.; Misra, A. Synthesis of an efficient pyrene based aie active functional material for selective sensing of 2,4,6-trinitrophenol. *J. Photochem. Photobiol. A Chem.* **2017**, *342*, 1–14. [[CrossRef](#)]
37. Palma, A.; Woitassek, D.; Brunklaus, G.; Scherf, U. Luminescent tetraphenylethene-cored, carbazole- and thiophene-based microporous polymer films for the chemosensing of nitroaromatic analytes. *Mater. Chem. Front.* **2017**, *1*, 1118–1124. [[CrossRef](#)]
38. Wang, G.Z.; Li, M.L.; Wei, Q.H.; Xiong, Y.H.; Li, J.; Li, Z.W.; Tang, J.Y.; Wei, F.; Tu, H.L. Design of an aie-active flexible self-assembled monolayer probe for trace nitroaromatic compound explosive detection. *ACS Sens.* **2021**, *6*, 1849–1856. [[CrossRef](#)]
39. Li, H.K.; Wu, H.Q.; Zhao, E.G.; Li, J.; Sun, J.Z.; Qin, A.J.; Tang, B.Z. Hyperbranched poly(aroxycarbonyltriazole)s: Metal-free click polymerization, light refraction, aggregation-induced emission, explosive detection, and fluorescent patterning. *Macromolecules* **2013**, *46*, 3907–3914. [[CrossRef](#)]
40. Wang, J.; Mei, J.; Yuan, W.Z.; Lu, P.; Qin, A.J.; Sun, J.Z.; Ma, Y.G.; Tang, B.Z. Hyperbranched polytriazoles with high molecular compressibility: Aggregation-induced emission and superamplified explosive detection. *J. Mater. Chem.* **2011**, *21*, 4056–4059. [[CrossRef](#)]
41. Yuan, W.Z.; Zhao, H.; Shen, X.Y.; Mahtab, F.; Lam, J.W.Y.; Sun, J.Z.; Tang, B.Z. Luminogenic polyacetylenes and conjugated polyelectrolytes: Synthesis, hybridization with carbon nanotubes, aggregation-induced emission, superamplification in emission quenching by explosives, and fluorescent assay for protein quantitation. *Macromolecules* **2009**, *42*, 9400–9411. [[CrossRef](#)]

Disclaimer/Publisher's Note: The statements, opinions and data contained in all publications are solely those of the individual author(s) and contributor(s) and not of MDPI and/or the editor(s). MDPI and/or the editor(s) disclaim responsibility for any injury to people or property resulting from any ideas, methods, instructions or products referred to in the content.